SUPPLEMENTING GROUND TRUTH DATA WITH SHEAR WAVE VELOCITY, SEISMIC ATTENUATION, AND THERMAL STRUCTURE OF THE CONTINENTAL LITHOSPHERE

Walter D. Mooney,[1] Irina Artemieva,[1,2] Shane T. Detweiler,[1] Magali Billien,[2] Jean-Jacques Leveque[2]

United States Geological Survey,[1] Ecole et Observatoire de Sciences de la Terre[2]

Sponsored by National Nuclear Security Administration
Office of Nonproliferation Research and Engineering
Office of Defense Nuclear Nonproliferation

Contract No. DE-A104-98AL79758

ABSTRACT

Ground truth data provide the opportunity to calibrate regional seismic velocity and Q (inverse attenuation) models. However, in many cases, available wave propagation data are too sparse to characterize seismic velocities and Q everywhere. It is therefore of interest to examine on a global basis the relationship between regional geology and heat flow versus the seismic properties (Vs and Qs) of the upper mantle. To better understand the propagation of seismic waves caused by nuclear explosions, we have developed new, theoretical models of the dissipation of energy in the crystalline rocks typical for the Earth's mantle. Using laboratory results, we suggest a temperature dependence of attenuation through the activation energy. We therefore compare maps of the thermal structure of the continental lithosphere with the inverse attenuation of seismic shear waves Qs and seismic velocity Vs as determined from surface wave dispersion and amplitudes. Our study is based on recently available global databases. We compare the values of Qs, Vs, and temperature T at the depths of 50, 100, and 150 km in the continental lithosphere. We find that qualitatively (by the sign of the anomaly) the maps of Qs closely correlate with lithospheric temperatures. The best correlation is observed for the depth of 100 km, where the resolution of the attenuation model is the highest. At this depth, the contour of zero attenuation anomaly approximately corresponds to the 1000^{o}C contour of lithospheric temperature, in agreement with laboratory data on a sharp change in seismic attenuation and shear velocities in upper mantle rocks at 900-1000^{o}C. The correlation between Vs and two other parameters (T and Qs), though present, is less distinct. We find that most cratonic regions show high lithospheric Vs, Qs and low T. Several prominent low Qs regions correlate with high lithospheric temperatures. We calculate that even if temperature variations in the lithosphere are the main cause of seismic velocity and attenuation variations, the relation between temperature and seismic properties is non-linear.

OBJECTIVE

It is widely accepted that a significant part of seismic velocity and attenuation anomalies in the mantle can be attributed to temperature variations. For the purposes of nuclear test monitoring at teleseismic distances, a knowledge of these anomalies is highly desirable. Ground truth data provide the opportunity to calibrate available regional seismic velocity and Q (inverse attenuation) models. However, in regions of interest such as Iran, India and China, wave propagation data are too sparse to adequately characterize seismic velocities and Q. It is therefore necessary that we examine on a global basis the correlations between seismic shear-wave velocities (V_s), inverse attenuation (Q_s), and temperature (T) in order to distinguish compositional and thermal origins of the attenuation anomalies in the upper mantle.

RESEARCH ACCOMPLISHED

Numerous seismic and laboratory studies have addressed the question of the correlation between seismic elastic and anelastic properties, and temperatures. (1) A global anelastic tomography study (Romanowicz, 1995) as well as regional seismic studies for the oceans (Sheehan and Solomon, 1992; Roth *et al,* 2000; Tsumura *et al,* 2000) found that **seismic velocity and attenuation** are correlated. (2) The strong effect of **temperature on seismic velocity** and elastic moduli was demonstrated by laboratory measurements (e.g., Berckhemer *et al,* 1982; Sato *et al,* 1989; Jackson *et al,* 1992; Jackson, 1993), implying that shear-wave velocity perturbations in the uppermost mantle can be caused by temperature variations. (3) The strong effect of **temperature on seismic attenuation** has been measured in a number of experimental studies. Laboratory measurements of seismic wave attenuation in ultramafic upper mantle rocks were carried out for a wide range of pressures and temperatures at ultrasonic frequencies (60-900 KHz) on dry peridotite (Sato *et al,* 1989) and at seismic frequencies (0.01-1 Hz) on dry dunite (Berckhemer *et al,* 1982; Jackson *et al,* 1992) and on synthetic polycrystalline olivine (Tan *et al,* 1997; Gribb and Cooper, 1998; Jackson, 2000). They show that at seismic frequencies attenuation, Q^{-1}, in mantle rocks at subsolidus temperatures follows the Arrhenius law and exponentially increases with temperature T:

$$Q^{-1} = T_o^{\alpha} \, exp\,(-\alpha E^*/RT), \qquad (1)$$

where E^* is the activation energy, R is the gas constant, T_o is the oscillation period, and the exponent α is about 0.15-0.30 as determined from seismic studies and laboratory measurements on the upper mantle rocks (e.g., Jackson *et al,* 1992).

Laboratory measurements with the temperature dependence of seismic attenuation were used in a number of studies where mantle geotherms were calculated from seismic attenuation (e.g., Kampfmann and Berckhemer, 1985; Sato *et al*, 1988; Sato and Sacks, 1989; Karato, 1990). The high sensitivity of seismic attenuation to temperatures, revealed in laboratory measurements, was used recently to correlate seismic attenuation anomalies in the mantle with temperature variations (e.g., Bodri *et al,* 1991; Durek *et al,* 1993; Mitchell, 1995; Romanowicz, 1994, 1995). Romanowicz (1995) found that in the depth interval from 100 to 300 km shear-wave attenuation Q_s^{-1} calculated from the amplitudes of low-frequency Rayleigh waves on a 10°x10° grid (the QR19 model) correlates with the surface heat flow values (the correlation coefficient r is in the range 0.20 to 0.35 with the correlation peak at z~200 km); while at depths of z>200 km Q^{-1} correlates with the hot spot distribution, with the strongest correlation (r~0.35–0.38) at z~300–660 km.

On the continents, low seismic attenuation in the upper mantle has been reported beneath western Australia, western Africa, and the Himalayas in a number of recent anelastic tomographic models (e.g. Romanowicz, 1994, Bhattacharyya *et al.,* 1996), supporting the idea of the thermal origin of most of the upper mantle Q_s anomalies. Seismic studies of shear-wave attenuation also revealed a qualitative correlation between regional attenuation anomalies in the crust and upper mantle and tectonic provinces (e.g., Nakanishi, 1978; Canas and Mitchell, 1978; Roult, 1982; Dziewonski and Steim, 1983; Chan and Der, 1988; Mitchell *et al,* 1997; Sarker and Abers, 1998).

Few studies have been carried out thus far to analyze: (a) the correlations between all three parameters (V_s, Q_s, and T) and (b) the global correlation between seismic attenuation and temperatures. We particularly know very little about regions where clandestine nuclear testing may be taking place. Here we present maps of V_s, Q_s, and T distributions at the depths of 50, 100, and 150 km and compare shear-wave velocities and attenuation at different depths in the upper mantle with temperature estimates in order to evaluate the influence of T on V_s and Q_s.

In the present study we use a subset of the 3-D V_s and Q_s models for the upper mantle produced by Billien (1999).

The models are based on the inversion of broadband seismological data of fundamental mode surface waves. The data used are amplitude and frequency spectra at periods between 40 s and 150 s for the direct path Rayleigh wave data (the first orbit) only, which is a subset of the extensive phase and amplitude data set measured and selected by Trampert and Woodhouse (2000). For a detailed description of the automatic measurement technique and implementation of the strict data rejection criteria, see Trampert and Woodhouse (1995).

V_s and Q_s calculations are based on a two-step inversion (for details see Billien, 1999; Billien *et al,* 2000). First, from phase (Φ) and amplitude (A) measurements, we made a simultaneous regionalization at several periods of the phase velocity (c_R) and the surface wave attenuation factor ($q_R=Q^{-1}{}_R$) (Billien *et al,* 2000):

$$A_i(\omega), \Phi_i(\omega) \Rightarrow c_R(\omega, \theta, \phi), q_R(\omega, \theta, \phi) . \quad (2)$$

A depth inversion of the phase velocity and surface wave attenuation maps at different frequencies provides a 3D model of the shear-wave velocity V_s and the shear-wave attenuation factor q_s ($q_s=Q_s^{-1}$) *(*Billien*,* 1999):

$$q_R(\omega, \theta, \phi) \Rightarrow q_s(z, \theta, \phi). \quad (3)$$

$$c_R(\omega, \theta, \phi) \Rightarrow V_s(z, \theta, \phi) \quad (4)$$

The classical inversion method of Tarantola and Valette (1982) is used at this stage. It employs a least-square method and includes information on the expected model in the form of: (1) an *a priori* model and (2) an *a priori* covariance of the model. Billien (1999) use a layered version of PREM with 50 km thick layers in the depth range 25 to 825 km as the *a priori* velocity and attenuation models. The upper 25 km ("the crustal layer") are fixed to the PREM value and are never updated in the inversion process. In the globally spherical PREM model (Dziewonski and Anderson, 1981) the radial average Q_s has a value of 600 at depths between 40 km and 80 km, and Q_s=80 between 80 km and 220 km. Similar to the attenuation model, the velocity value in the "crustal layer" is not allowed to change in the inversion, since the phase velocity maps are corrected at all periods for the crustal effects calculated from the CRUST5.1 model (Mooney *et al,* 1998). These corrected maps as a function of period are then inverted to obtain the 3D *S*-velocity model.

The *a priori* covariance of the attenuation model is described by *a priori* standard deviations as a function of depth. In order to allow larger Q_s variation in the lithosphere, which is believed to be more heterogeneous than the asthenosphere, a standard deviation on the *a priori* model σ_m was chosen to be twice as large in the lithosphere as in the asthenosphere.

The results for Q_R, and hence for Q_s, account for the effect of focusing (due to velocity heterogeneities) on the wave amplitude. More precisely, a linear approximation (Woodhouse and Wong, 1986) is used to include the focusing effect in the inversion. Amplitude variations due to scattering are not separately modeled. Thus the attenuation factor derived in this study includes both anelastic and scattering effects.

In the regionalization, smooth models were favored over rough models. This is achieved by use of a cost function based on the norm of the Lagrangian (second derivatives) of the model (Billien *et al,* 2000) rather than a classical damped least square method based on the norm of the model (e.g., Tarantola and Valette, 1982). In our model, phase velocity and attenuation maps, and then V_s and Q_s maps, are represented by spherical harmonics up to degree l=20. However, the effective degree of the computed maps is only 12 to 13, due to the damping used in the regionalization that progressively shut off the highest degree terms. This effective degree corresponds to a ~3000 km wavelength of attenuation and velocity lateral variations.

The depth resolution matrix shows that the best resolved layer for Q_s is at a depth of 100±25 km. The tuning of the cost function in the first step of the inversion largely influences the absolute values of Q_R variations (Billien *et al*, 2000) and thus the values of Q_s, but the sign of the variations and the sharpness of the contrasts are less sensitive to this tuning. Moreover, due to large perturbations found for attenuation, the numerical values are sensitive to the choice of the displayed parameters, $\Delta Q_s/Q_s$ or $-\Delta Q_s^{-1}/Q_s^{-1}$. For instance, our choice to display $-\Delta Q_s^{-1}/Q_s^{-1}$ anomalies (Figures 1-3) leads to perturbation values in the range between -250% and +100%. Plotting $\Delta Q_s/Q_s$ anomalies would lead to the same figure, but with perturbations ranging from -71% to 0. Since Billien (1999) and Billien *et al* (2000) use a damped inversion, the value of Q_s variations at each depth layer within the lithosphere is probably underestimated. On the whole, the vertical resolution of V_s and Q_s models is ~50 km.

Two global studies of the thermal regime of the continental lithosphere are available at present. The model of Pollack and Chapman (1977) is based on a degree-12, spherical harmonic representation of global surface heat flow and provides a rather generalized estimate of lithospheric thickness. Since that study numerous new heat flow measurements have become available. Here we use a more recent global model of the thermal state of the continental lithosphere (Artemieva and Mooney, 2001), hereafter referred to as the AM01 model. The model is based on global heat flow database (Pollack *et al,* 1993) updated for more recent heat flow measurements reported since 1993, and crustal structure database (Mooney *et al,* 1998, 2002). Estimates of the thermal regime of the stable continental lithosphere are based on the solution of the steady-state thermal conductivity equation:

$$\nabla^2 T = - A/k \quad (5)$$

with the boundary conditions at the surface given by:

$$T \big|_{z=0} = 0 \quad (6)$$

$$q_0 = - k \, \partial T/\partial z \quad (7)$$

where q_0 is the near-surface heat flow, T is temperature, $k = k(z)$ and $A = A(z)$ are thermal conductivity and the heat production as functions of depth. The solution of Eqs. (5)–(7) permits the calculation of temperatures within the crust and lithospheric mantle, constrained by borehole heat flow measurements, q_0, (Pollack *et al,* 1993) and the distribution of thermal parameters with depth.

The strong effect of temperature on seismic velocities is known from laboratory studies (e.g. Berckhemer *et al,* 1982; Kampfmann and Berckhemer, 1985; Sato *et al*, 1989). A number of studies where upper mantle temperatures are estimated from seismic velocities (e.g. Sobolev *et al,* 1996; Goes *et al,* 2000; Goes and van der Lee, 2002) assume the existence of a strong correlation between these parameters. However, for the maps presented in Figures 1, 2, and 3, a statistical analysis of the correlation (r) between V_s and T in the lithospheric mantle of the continents suggests that even though there is the expected negative correlation between the two parameters (r=-0.38 at z=100 km and r=-0.42 at z=150 km) (Table 1), the conversion of seismic velocities into temperatures (or visa versa) is subject to considerable uncertainty. For a depth of 100 km, the range of possible temperatures corresponding to any given velocity value is at least ±250^o C. At shallower depth (50 km) almost no correlation exists between V_s and T due to a large scatter in both of the parameters.

A qualitative correlation between seismic attenuation and velocities that has been observed in regional (e.g., Sheehan and Solomon (1992) and Tsumura *et al* (2000)) and global studies (Romanowicz, 1995), suggests to relate these two parameters quantitatively. Such an attempt was recently made by Roth *et al* (2000) for the Fiji-Tonga region, which assumed that anomalies of both attenuation and velocities have a similar thermal origin. They find that, at depths greater than 100 km, velocity and attenuation anomalies are strongly correlated and can be fit by an exponential equation; at shallower depths their data show a high degree of scattering.

Roth *et al* (2000) also examined the correlation between attenuation and shear-wave velocity anomalies derived from global seismic tomography studies (Su *et al,* 1994; Romanowicz, 1995) and concluded that the strong correlation between Q_s and V_s, observed in the Tonga subduction zone is more a regional phenomenon than a general rule. The statistical analysis of a global Q_s -V_s dataset for the continents presented here (Table 1) supports this conclusion. However, the correlation between Q_s and V_s varies with tectonic provinces. In accord with the results of Roth *et al* (2000), we do observe poor correlation (r=0.38) between Q_s and V_s in shallow (50 km) lithosphere of the continents, probably because crustal effects have the greatest influence on calculated Q_s and V_s at 50 km depth. However, the correlation remains low at 100-150 km depth, even though in this depth interval scattering has a lesser effect on Q_s.

The influence of temperature on seismic attenuation was examined in a number of laboratory experiments, where an exponential law for the correlation of two parameters was found (Berckhemer *et al,* 1982; Kampfmann and Berckhemer, 1985; Sato *et al*, 1989; Jackson *et al,* 1992; Gribb and Cooper, 1998). The only attempt to calculate temperatures from seismic attenuation data that we are aware of is presented by Sarker and Abers (1999) for the crust of southern and central Eurasia. Though regional seismic data show the existence of a correlation between deep temperatures and attenuation (e.g. Bodri *et al,* 1991), statistical analysis (Table 1) shows that in reality the coefficient of correlation is, in general, weak (r=-0.34 at z=150 km).; at shallower depths no significant correlation is observed on the global scale (r~0.2).

A poor correlation between Q_s and T suggest that effects other than temperature (e.g., composition, fluids, partial melt) play an important role in producing attenuation anomalies in the upper mantle. For example, in stable continental regions one would expect that compositional variations could play a dominant role in smearing the correlation between Q_s and T; for example, at 100 km depth, temperatures of 800-900^o C can exist in both Paleozoic and Precambrian platforms (Artemieva and Mooney, 2001). At the same time, petrological studies (e.g. Boyd, 1989) indicate that subcrustal lithosphere of the Precambrian cratons is chemically depleted compared to oceanic lithosphere and younger platforms and has higher Mg/Fe ratio. No experimental studies have examined how depletion can influence seismic attenuation. However, recent laboratory measurements of attenuation in MgO (Getting *et al,* 1997) suggest that variations in Mg in the subcrustal lithosphere of the cratons and Paleozoic platforms could affect seismic attenuation values.

We next qualitatively compare maps of seismic and temperature anomalies in the upper mantle to examine if there is a qualitative agreement between the parameters and to check if the quantitative correlation does not hold due to high amplitude variations of seismic anomalies at near-solidus temperatures. The maps of shear-wave velocity V_s, shear-wave quality factor Q_s, and temperature T are plotted at three depths (Figures 1-3). Due to the vertical resolution of V_s and Q_s models, the velocity and attenuation maps refer to depth intervals of 50±25 km, 100±25 km, and 150±25 km.

We emphasize a comparison of V_s, Q_s, and T maps only for the continental regions where an acceptable resolution is achieved for all three parameters. In this section we discuss only the qualitative correlations of the anomalies, and Figures 1-3 reveal the existence of a strong overall qualitative correlation between the signs of V_s, Q_s, and T anomalies for most of the continental lithosphere at depths of 50-150 km (see also Table 2). At first look, there is less correlation between the three maps for a depth of 150 km. The eye catches strong positive seismic anomalies over North America and Eurasia, while temperature anomalies appears to be much weaker there. However, a more careful comparison of the maps reveals a good qualitative correlation between the signs of the anomalies at this depth as well (see Table 2 for summary). The correlation (in terms of the sign of the anomalies) between the T and Q_s for most of the continents suggests that the anelasticity anomalies in the continental lithosphere are primarily caused by thermal effects.

Table 2 gives a summary of the qualitative comparison of shear-wave velocity, inverse shear-wave attenuation and temperature anomalies for the continents. It shows that in most tectonic provinces the signs of all three anomalies are well correlated; however in some regions only two types of the anomalies correlate.

There are two types of regions where all three anomalies correlate. “Cold” regions include most of the Precambrian cratons; “hot” regions include continental rifts, Cenozoic orogens and, unexpectedly, the Sino-Korean craton. A correlation between the signs of all three anomalies is observed within both of the groups throughout the entire lithosphere and suggests a thermal origin of most of the seismic anomalies.

“Hot” (red) anomalies (low V_s, low Q_s, and high T) are found in all three maps (Figure 1) for many tectonically active regions of the continents, that includes western North America (which is largely composed of young accreted terrains), the Andes, Cenozoic eastern Australia, the Red Sea rift, and Phanerozoic western Europe. However, some active tectonic regions show a non-correlated behavior of the anomalies, which will be discussed below.

At all depths, blue, “cold” anomalies with high V_s, high Q_s, and low T dominate in cratonic regions (see Table 2 for a summary). This includes the Canadian shield, the Siberian craton, the Baltic shield and the East European platform, the Precambrian Western Australia, and the Indian craton. It is possible that Greenland is also characterized by the “cold” set of V_s, Q_s and T anomalies; however, the velocity and attenuation anomalies are smeared due to the proximity of the Icelandic plume. The Brazilian shield of South America shows a correlation of high V_s with high Q_s, but T estimates are absent there, except for the Saõ-Francisco craton, which is characterized by low T typical for the cratonic lithosphere.

On the whole, we find a better agreement between T and Q_s for large cratons than for small ones. Large cratons (the Canadian shield, the Baltic shield, the East European platform, and the Siberian craton) have lower attenuation and lower temperature down to at least 200-250 km depth (and even deeper for attenuation anomalies *(*Billien*,* 1999)), implying that cold, thick lithosphere beneath these Precambrian cratons is present to at least this depth (c.f., Jordan,

1988; Nyblade and Pollack, 1993; Artemieva and Mooney, 2001). Since T and Q_s are so well correlated, we suggest that attenuation maps can provide a first order estimate of lithospheric temperatures in regions where the heat flow measurements are sparse.

A strong correlation between all three anomalies, V_s, Q_s, and T, is observed at 100 km depth beneath most of Eurasia, with the strongest anomalies beneath the Baltic shield and East European platform and beneath the Siberian craton, which are separated by a "hot" high-temperature and high-attenuation anomaly beneath the much younger West Siberian basin. However, at 150 km depth, a pronounced "cold" attenuation anomaly in the West Siberian basin (Figure 3b) is not correlated with high temperature anomaly (Figures 3c). At 150 km depth, northern Eurasia is another large region with poorly correlated temperature and attenuation anomalies, though it displays a somewhat better correlation between shear velocities and temperatures.

The nuclear test monitoring community has a number of regions of potential interest. We examine one, China, in detail here. The Early Proterozoic Sino-Korean craton, which has undergone intensive tectonic reworking since the late Mesozoic, shows near-zero anomalies in the three maps at 100 km depth and "hot" anomalies in the maps for 150 km. Surface heat flow data suggest that the lithosphere there is atypically thin (120-150 km, Artemieva and Mooney, 2001) compared to other cratons and lithospheric temperatures are intermediate between other Precambrian cratons and tectonically active Cenozoic regions. Xenolith studies (Griffin et al, 1998) provide evidence that the composition of the lithosphere of the Sino-Korean craton has been significantly modified by Mesozoic-Cenozoic tectonic and magmatic activity, and that its lower part (below 80-140 km depth) has been largely or even completely removed and replaced by more fertile Phanerozoic material (Xu *et al,* 2000). Thus, a part of V_s and Q_s variations there may probably have a non-thermal origin.

The Tibet-Himalayan orogen is consistently evident only in the map of T. However, temperature estimates in the lithosphere of this region are not calculated from the surface heat flow data, but were derived from petrological and non-steady state model constraints (e.g., Henry *et al,* 1997), and thus should be interpreted with caution. Moreover, the existence of a large time delay in the upward propagation of a thermal anomaly also implies that the correlation between seismic models and geotherms derived from surface heat flow data should be the best in stable regions that did not undergo tectonic or magmatic activity over a long geological time. The cratonic regions are the best examples of such structures and, as discussed above, indeed show a strong correlation between seismic parameters, on one hand, and the thermal state, on the other hand. Though orogenic regions like the Himalayas are not expected to closely follow the same rule, we cannot identify any region where seismic anomalies are clearly of a non-thermal origin.

The regions with non-correlated seismic anomalies in the lithosphere deserve special attention, as both V_s or Q_s anomalies used in this study were derived in a joint inversion of one data set (Billien, 1999; Billien *et al,* 2000). However, according to experimental studies on polycrystalline olivine at seismic frequencies (e.g. Jackson, 2000), attenuation in shallow lithosphere needs not correlate with temperature and shear-wave velocities, because at low T ($<600^o$ C) typical for shallow cratonic lithosphere the upper mantle rocks exhibit an almost elastic behavior, while the values of Q^{-1} are essentially scattered.

The Alpine-Himalayas zone, which extends from the Alps through the Asia Minor to the Tibetan Plateau, clearly appears in Figures 1b and 1c as a hot and highly attenuating zone. However, the V_s anomaly is close to zero at all depths, rather than showing the expected negative anomaly. Other regions where neither Q_s nor T anomalies correlate with V_s anomalies in the deep lithosphere (z~100-150 km) include the West Siberia basin and the Arabian shield. However, the lateral dimensions of the Arabian shield are too small to be resolved by the seismic models used in the present study. In the West Siberia basin, the disagreement between Q_s and T may also be apparent due to a very high amplitude of attenuation anomaly beneath the Siberian craton in East Siberia, which may possibly "overprint" attenuation anomaly in the basin (~2000 km from east to west compared to the lateral resolution of the seismic models of ~3000 km).

On the other hand, laboratory and theoretical studies (e.g., Berckhemer *et al,* 1982; Karato and Spetzler, 1990; Jackson *et al,* 1992) indicate that seismic attenuation is considerably more sensitive to temperature variations than elastic velocities, while seismic velocities are to a larger degree affected by compositional variations (e.g., Bina and Silver, 1997; Deschamps *et al,* 2002). We, therefore, favor a compositional origin of the velocity anomalies beneath the West Siberia basin. This conclusion is supported by the results of the recent study of Kaban *et al* (2002), in

which lithospheric gravity anomalies were corrected for temperatures in order to discriminate between compositional and thermal effects. One of the conclusions of that study is that there are large compositional differences between the Precambrian lithospheres of the East European platform and the Siberian craton, on one hand, and the Paleozoic West Siberian basin, on the other hand. As seismic attenuation in the cratonic lithosphere seem to have purely thermal origin, a compositional origin of seismic anomalies in the lithosphere of West Siberian basin cannot be ruled out.

CONCLUSIONS AND RECOMMENDATIONS

We examine the correlations among seismic shear-wave velocity, Q_s, and temperature in order to distinguish the attenuation anomalies in the upper mantle of thermal origin. Our analysis is based on the shear-wave velocity and shear-wave attenuation anomalies in the lithosphere, calculated for the whole Earth from the broad-band seismological data of the fundamental mode surface waves at periods 40 to 150 sec (Billien, 1999; Billien *et al,* 2000), and on the data on lithospheric temperatures beneath continents (Artemieva and Mooney, 2001).

1. We present a qualitative comparison of V_s, Q_s, and T lithospheric anomalies based on the visual comparison of the maps for 50, 100, and 150 km. A weak visual correlation at 50 km depth between seismic parameters and temperature can be attributed to the low resolution of V_s and Q_s at shallow depth due to the sensitivity to the corrections for crustal effects.

At depths of 100 and 150 km, high V_s, high Q_s, and low T correlate with cratons, except for the South America and South Africa, where seismic anomalies may be artifacts produced by smearing of offshore anomalies. We propose that positive seismic anomalies in the cratonic lithosphere are primarily of the (low-T) thermal origin. Correlation between attenuation and temperature anomalies in the cratonic lithosphere can be used to estimate lithosphere thickness in the regions where heat flow measurements are absent.

Similarly, we find the expected inverse correlations (low V_s, low Q_s, and high T) for many tectonically active regions. We hypothesize that fluids, partial melts, or compositional anomalies can have an essential effect on anelastic and elastic seismic properties of the continental lithosphere.

2. Comparison of the attenuation values calculated from seismic inversion with theoretical estimates based on temperatures and analytical equations derived in laboratory studies (Sato and Sacks, 1989; Jackson *et al*, 1992) suggests that attenuation can be considered as an indicator of tectonic processes only in the upper 100 km of the lithosphere.

3. This study shows that even if temperature variations in the lithosphere are the main cause of seismic velocity and attenuation variations, the relation between temperature and seismic properties is non-linear and the hypothesis of compositionally homogeneous lithospheric roots is invalid. Rather, the lithospheric mantle appears to have a complex deep structure, analogous to the crust. These compositional and structural variations contribute to the observed anomalies in seismic properties.

For the purposes of nuclear test monitoring, we believe that we have developed a new method for supplementing ground truth data by providing calibrations of regional seismic velocity and Q (inverse attenuation) for regions of interest. Additional wave propagation data where data are currently sparse would be useful as a check of this new method. However, results indicate that our models are very useful for detection and monitoring of the propagation of seismic waves caused by nuclear explosions. We recommend that further implementation of this technique be considered.

Table 1. Correlation coefficients between temperature, seismic velocity, and attenuation for different upper mantle depths

Depth	T vs Q_s	T vs V_s	V_s vs Q_s
50 km	-0.19	-0.19	0.38
100 km	-0.23	-0.38	0.41
150 km	-0.34	-0.42	0.41
200 km	-0.23	-0.26	0.25

Table 2. Qualitative correlations between Vs, Qs and T for different tectonic provinces

Depth	V_s, Q_s and T correlate	V_s and Q_s do not correlate with T	V_s and T do not correlate with Q_s	Q_s and T do not correlate with V_s
50 km	cratons, Ar-ePt ("cold"): 1. Canadian shield 2. Baltic shield 3. East European Platf. 4. Siberian craton 5. Western Australia 6. Indian shield 7. Greenland ? 8. Amazonian craton? Active regions, Cz-Pz ("hot"): 1. Western North America 2. the Andes 3. Eastern Australia 4. Western Europe 5. Alpine-Himalayan belt (V_s anomaly weak)	1. East African Rift, Cz (hot T, cold V_s and Q_s) 2. Sino-Korean craton, ePt/Mz (hot V_s and Q_s, cold T)	1. West African craton, Ar-ePt (cold V_s and T, Q_s~0) 2. South Africa, Ar-ePt (cold V_s and T, hot Q_s)	1. West Siberian basin, Pz (hot Q_s and T, cold V_s) 2. Arabian shield, m-lPt (cold Q_s and T, hot V_s)
100 km	cratons, Ar-ePt ("cold"): 1. Canadian shield 2. West African craton 3. Baltic shield 4. East European Platf. 5. Siberian craton 6. Western Australia 7. Greenland ? 8. Amazonian craton ? 9. Congo craton ? Active regions, Cz-Pz ("hot"): 1. Western North America 2. the Andes 3. Eastern Australia 4. Western Europe 5. Alpine-Himalayan belt (V_s anomaly weak) Intermediate anomalies: 1. Sino-Korean craton, ePt/Mz (V_s~0, Q_s and T variable)	1. East African Rift, Cz (hot T, cold V_s and Q_s)	1. South Africa, Ar-ePt (cold V_s and T, hot Q_s) 2. Indian shield, Ar-ePt (cold V_s and T, hot Q_s)	1. West Siberian basin, Pz (hot Q_s and T, cold V_s) 2. Arabian shield, m-lPt (cold Q_s and T, V_s ~0) 3. Amazonian craton, Ar-ePt (hot Q_s and T, cold V_s)
150 km	cratons, Ar-Pt ("cold"): 1. Canadian shield	1. Tibet and Himalayas, ePt-Cz	1. Baltic shield, Ar-Pt (cold V_s and T, Q_s ~0)	1. East African Rift, Cz (hot Q_s and T,

	2. East European Platf. 3. Siberian craton 4. West African craton 5. Western Australia 6. Arabian shield 7. Greenland ? <u>cratons, Ar-ePt (zero anomalies):</u> 1. Indian shield 2. Amazonian craton? <u>Active regions, Cz-Pz ("hot"):</u> 1. Western North America 2. the Andes 3. Eastern Australia 4. Western Europe 5. Sino-Korean craton, ePt/Mz 6. Red Sea rift and Afar	(hot T, cold V_s and Q_s) 2. West Siberian basin, Pz (all three parameters poorly correlate: hot T, cold Q_s, and V_s ~0)	2. South Africa, Ar-ePt (cold V_s and T, hot Q_s)	cold V_s)

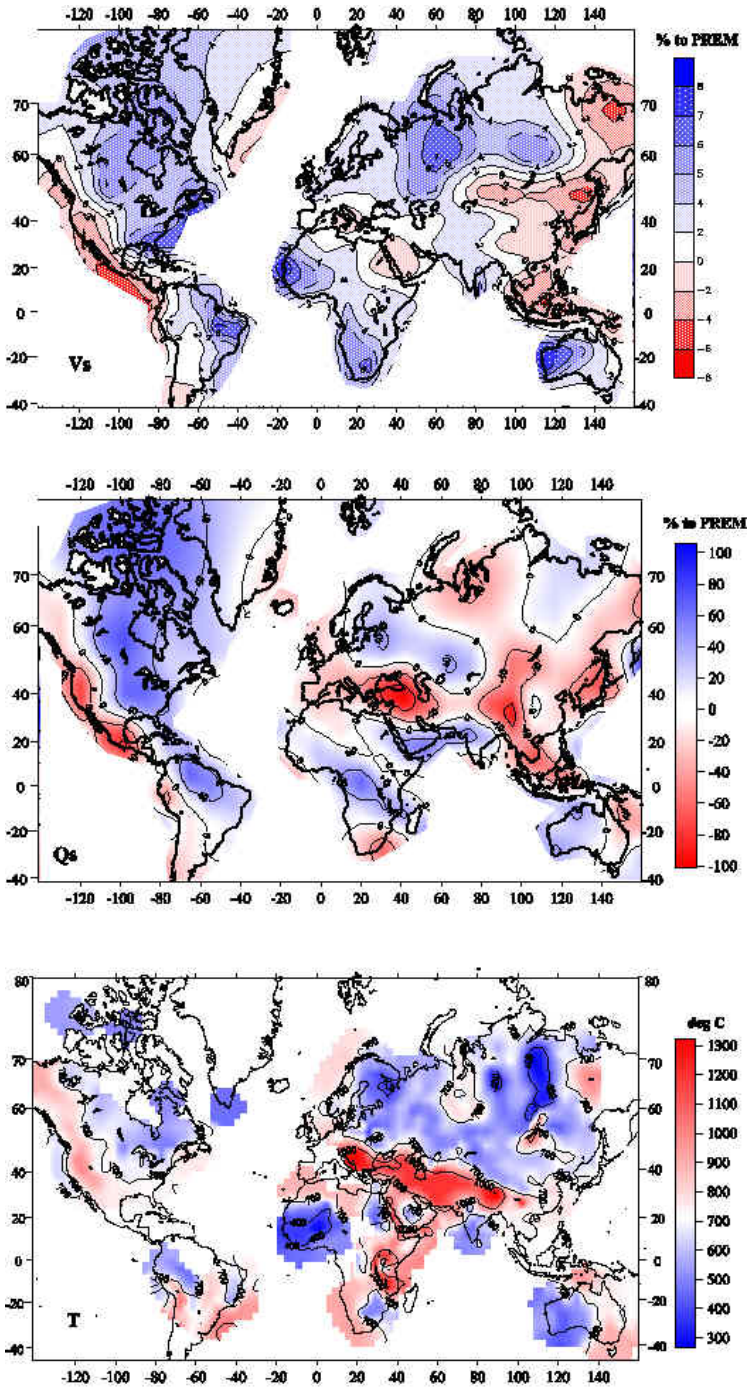

Figure 1. Map of shear-wave velocity V_s (as variation in % to PREM), inverse attenuation Q_s (as variation in % to PREM, $-\Delta Q_s^{-1}/Q_s^{-1}$), and temperature T (in deg C) for continental lithosphere at a depth of 50 km. Blue colors correspond to high V_s, high Q_s, and low T. Red colors correspond to low V_s, low Q_s, and high T. The dominant pattern on all three maps is the correlation of blue colors with stable Precambrian cratons and red colors with tectonically active Phanerozoic regions. The maps show a correlation in blue regions in the Canadian, Baltic, Siberian, West African, and Australian cratons. Red regions that correlate include western North America, Europe, the Middle East, eastern China and eastern Australia.

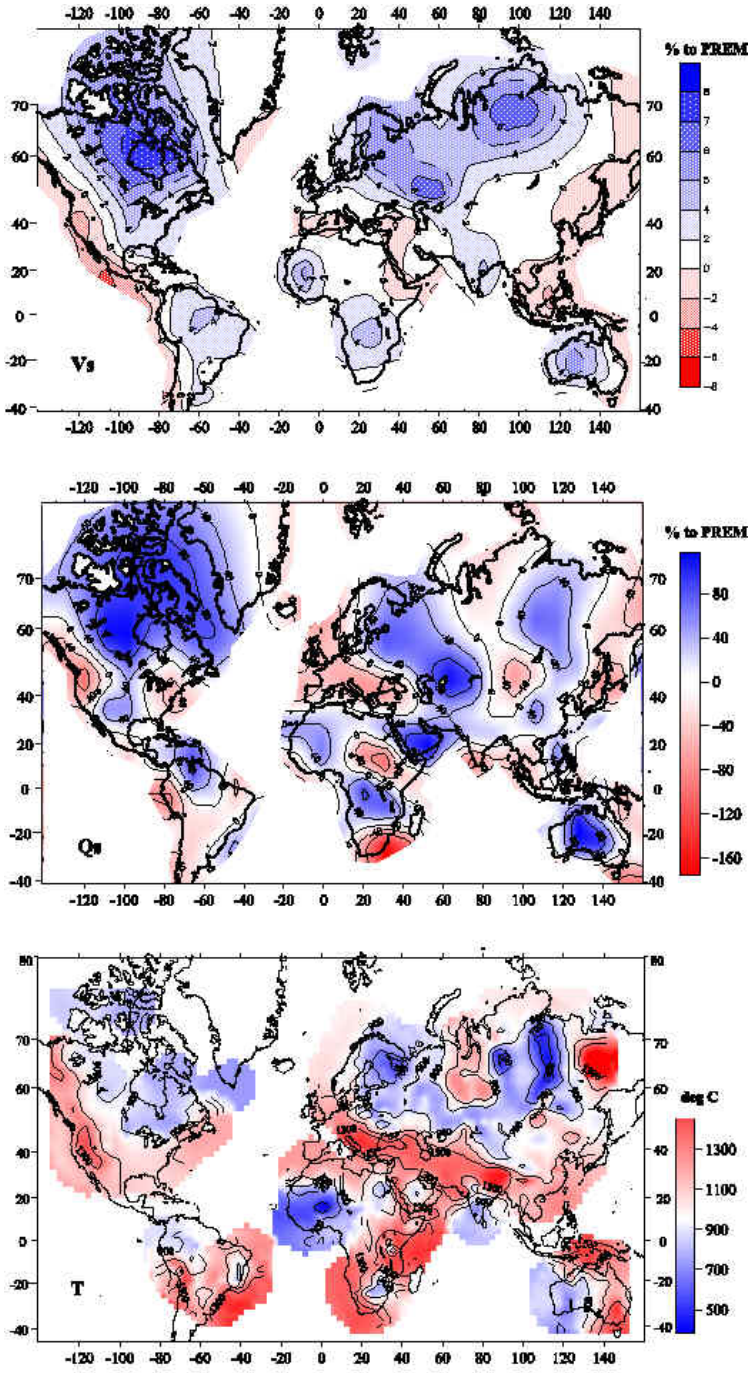

Figure 2. Map of shear-wave velocity V_s (as variation in % to PREM), inverse attenuation Q_s (as variation in % to PREM), and temperature T (in deg C) for continental lithosphere at a depth of 100 km. Presentation as in Figure 1. There is a close correspondence in the anomaly patterns for most of the Precambrian cratons and the Cenozoic regions, especially for the Precambrian Eurasia, West Africa, northern Canada, western North America and central Australia. This correspondence indicates that temperature plays the dominant role in determining the strength of V_s and Q_s anomalies at this depth in the lithosphere.

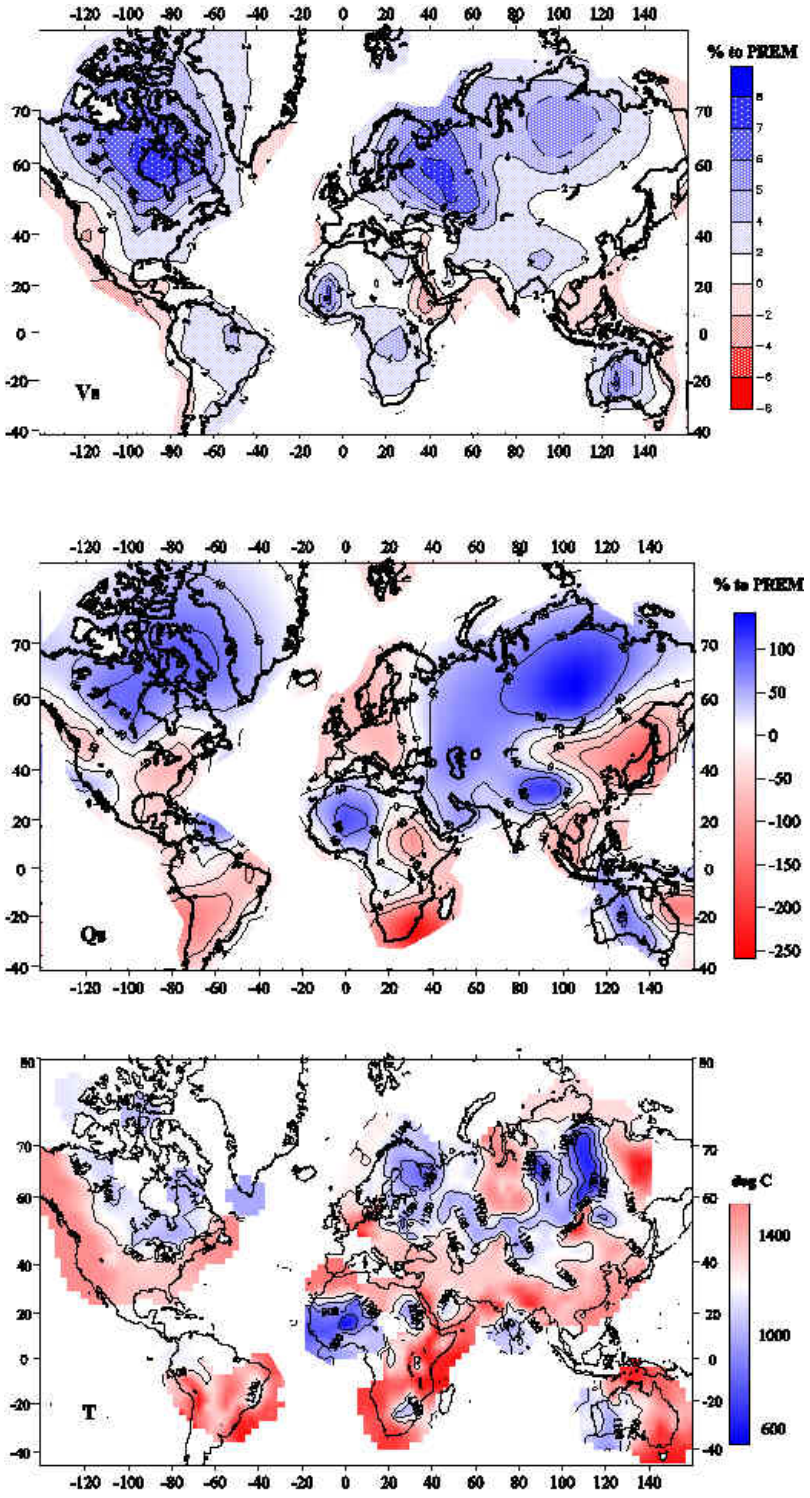

Figure 3. Map of shear-wave velocity V_s (as variation in % to PREM), inverse attenuation Q_s (as variation in % to PREM), and temperature T (in deg C) for continental lithosphere at a depth of 150 km. Presentation as in Figure 1. All low temperatures (lower panel) correspond to stable cratons. In contrast, high V_s and high Q_s anomalies include these same stable cratons plus some regions of active tectonics, such as the southern Eurasia suture zone extending from the Alps to the Tibetan plateau. This may indicate the presence of cold subducted lithosphere beneath the southern European suture zone.

REFERENCES

Artemieva I.M. and Mooney W.D., 2001. Thermal structure and evolution of Precambrian lithosphere: A global study. *J. Geophys. Res,* 106, 16387-16414.

Berckhemer H., Kapfmann W., Aulbach E., and Schmeling H., 1982. Shear modulus and Q of forsterite and dunite near partial melting from forced oscillation experiments. *Phys. Earth Planet. Interiors,* 29, 30-41.

Bhattacharyya J.G., Masters G., and Shearer P.,1996. Global lateral variations of shear attenuation in the upper mantle. *J. Geophys. Res.,* 101, 22273-22290.

Billien M., 1999. Hétérogénéités de vitesse et d'attenuation du manteau superior à l'echelle globale par modelisation du mode fundamental des ondes de surface. *PhD Thesis*, EOST-IPG, Strasbourg.

Billien M., Lévêque J.-J., and Trampert J., 2000. Global maps of Rayleigh wave attenuation for periods between 40 and 150 seconds. *Geophys. Res. Lett*., 27, 3619-3622.

Bina C.R. and Silver P.G., 1997. Bulk sound travel times and implications for mantle composition and outer core heterogeneity. *Geophys. Res. Lett*., 24, 499-502.

Bodri B., Iizuka S. and Hayakawa M., 1991. Relations between deep temperatures and other geophysical characteristics in central Honshu, Japan. *Tectonophys.,* 194, 325-336.

Boyd F.R., 1989. Compositional distinction between oceanic and cratonic lithosphere. *Earth Planet. Sci. Lett.,* 96, 15-26.

Canas J.A. and Mitchell B.J., 1978. Lateral variation of surface wave anelastic attenuation across the Pacific. *Nature,* 328, 236-238.

Chan W.W. and Der Z.A., 1988. Attenuation of multiple ScS in various parts of the world. Geo*phys. J*., 92, 303-314.

Deschamps F., Trampert J., and Snieder R., 2002. Anomalies of temperature and iron in the uppermost mantle inferred from gravity data and tomographic models. *Phys. Earth Planet. Inter*., 129, 245-264.

Durek J.J., Ritzwoller M.H. and Woodhouse J.H., 1993. Constraining upper mantle anelasticity using surface wave amplitude anomalies. *Geophys. J. Int.,* 114, 249-272.

Dziewonski A. and Steim J., 1983. Dispersion and attenuation of mantle waves through waveform inversion. *Geophys. J. Roy. Astron. Soc*., 70, 503-527.

Dziewonski A.M. and Anderson D.L., 1981. Preliminary reference Earth model. *Phys. Earth Planet. Inter.*, 2, 297-356.

Getting I.C., Dutton S.J., Burnley P.C., Karato S. and Spetzler H.A., 1997. Shear attenuation in and dispersion in MgO. *Phys. Earth Planet. Inter.,* 99, 249-257.

Goes S., Govers R., and Vacher P., 2000. Shallow mantle temperatures under Europe from P and S wave tomography. *J. Geophys. Res.,* 105, 11153-11169.

Goes S. and van der Lee S., 2002. Thermal structure of the North American uppermost mantle inferred from seismic tomography. *J. Geophys. Res.,* 107(B3).

Gribb T.T. and Cooper R.F., 1998. Low-frequency shear-attenuation in polycrystalline olivine: Grain boundary diffusion and the physical significance of the Andrade model for viscoelastic rheology. *J. Geophys. Res.,* 103, 27267-27279.

Griffin W.L., Zhang A., O'Reilly S.Y., and Ryan C.G., 1998. Phanerozoic evolution of the lithosphere beneath the Sino-Korean craton. In: Flower M. et al. (Eds.), Mantle dynamics and plate interactions in East Asia. Washington, D.C., *AGU Geodynam. Monogr*. 27, 107-126.

Henry P., Le Pichon X., and Goffe B., 1997. Kinematic, thermal and petrological model of the Himalayas: constraints related to metamorphism within the underthrust Indian crust and topographic elevation. *Tectonophys*., 273, 31-56.

Jackson I., 1993. Progress in the experimental study of seismic wave attenuation. *Ann. Rev. Earth Planet. Sci.,* 21, 375-406.

Jackson I., Paterson M.S., Fitz Gerald J.D., 1992. Seismic wave dispersion and attenuation in Åheim dunite: an experimental study. *Geophys. J. Int.,* 108, 517-534.

Jackson I., 2000. Laboratory measurement of seismic wave dispersion and attenuation: recent progress. *Geophysical Monograph,* 117, 265-289.

Jordan, T.H., 1988. Structure and formation of the continental tectosphere. *J. Petrology*, 29, 11-37.

Kaban M.K., Schwintzer P., Artemieva I.M., and Mooney W.D., 2002. Density of continental roots: compositional and thermal effects. *Earth Planet. Sci. Lett.(submitted).*

Kampfmann W. and Berckhemer H., 1985. High temperature experiments on the elastic and anelastic behaviour of magmatic rocks. *Phys. Earth Planet. Inter.,* 40, 223-247.

Karato S.-I., 1990. Low Q zone at the base of the mantle: Evidence for lower mantle convection? *Phys. Earth Planet. Inter*., 22, 155-161.

Karato S.I. and Spetzler H.A., 1990. Effect of microdynamics in minerals and solid-state mechanisms of seismic wave attenuation and velocity dispersion in the mantle. *Rev. Geophys*., 28, 399-421.

Mitchell B.J., 1995. Anelastic structure and evolution of the continental crust and upper mantle from seismic surface wave attenuation. *Rev. Geophys.,* 33, 441-462.

Mitchell B.J., Pan Y., Xie J. and Cong L., 1997. Lg coda Q variation across Eurasia and its relation to crustal evolution. *J. Geophys. Res.,* 102, 22767-22779.

Mooney W.D., Laske G., and Masters T.G., 1998. CRUST 5.1: A global crustal model at 5^{o}x5^{o}. *J. Geophys. Res.,* 103, 727-747.

Mooney, W.D., Prodehl, C., and Pavlenkova, N.I., 2002. Seismic velocity structure of the continental lithosphere from controlled source data. In: H. Kanamori, P. Jennings, and W.H.K. Lee (Eds.): *IASPEI Handbook on Earthquake and Engineering Seismology*, Academic Press, San Francisco, p. 887-910.

Nakanishi I., 1978. Regional difference in the phase velocity and the quality factor Q of mantle Rayleigh waves. *Science,* 200, 1379-1381.

Nyblade A.A. and Pollack H.N., 1993. A global analysis of heat flow from Precambrian terrains: Implications for the thermal structure of Archean and Proterozoic lithosphere. *J. Geophys. Res*., 98, 12207-12218.

Pollack H.N. and Chapman D.S., 1977. On the regional variation of heat flow, geotherms and lithospheric thickness. *Tectonophys*., 38, 279-296.

Pollack H.N., Hurter, S.J., and Johnson, J.R., 1993, Heat flow from the Earth's interior: analysis of the global data set. *Rev. Geophysics,* 31, 267-280.

Romanowicz B., 1994. Anelastic tomography: a new perspective on upper-mantle thermal structure. *Earth Planet. Sci. Lett.,* 128, 113-121.

Romanowicz B., 1995. A global tomographic model of shear attenuation in the upper mantle. *J. Geophys. Res*., 100, 12375-12394.

Roth E.G., Wiens D.A. and Zhao D., 2000. An empirical relationship between seismic attenuation and velocity anomalies in the upper mantle. *Geophys. Res. Lett., 27*, 601-604.

Roult G., 1982. The effect of young oceanic regions on the periods and damping of free oscillations of the Earth. *J. Geophys.,* 51, 38-43.

Sarker G. and Abers G.A, 1998. Deep structures along the boundary of a collisional belt: attenuation tomography of P and S waves in the Greater Caucasus. *Geophys. J. Int.,* 133, 326-340.

Sarker G. and Abers G.A., 1999. Lithospheric temperature estimates from seismic attenuation across range fronts in southern and central Eurasia. *Geology,* 27, 427-430.

Sato H.I., Sacks E., Takahashi E., and Scarfe C.M., 1988. Geotherms in the Pacific Ocean from laboratory and seismic attenuation studies. Nature, 336, 154-156.

Sato H., Sacks I.S., 1989. Anelasticity and thermal structure of the oceanic mantle: Temperature calibration with heat flow data. *J. Geophys. Res.,* 94, 5705-5715.

Sato H., Sacks I.S., Murase T., Muncill G., and Fukuyama H., 1989. Q_p-melting temperature relation in peridotite at high pressure and temperature: Attenuation mechanism and implications for the mechanical properties of the upper mantle. *J. Geophys. Res.*, 94, 10647-10661.

Sheehan A.F. and Solomon S.C., 1992. Differential shear wave attenuation and its lateral variation in the North Atlantic region. *J. Geophys. Res.,* 97, 15,339-15,350.

Sobolev S.V., Zeyen H., Stoll G., Werling F., Altherr R. and Fuchs K., 1996. Upper mantle temperatures from teleseismic tomography of French Massif Central including effects of composition, mineral reactions, anharmonicity, anelasticity and partial melt. *Earth Planet. Sci. Lett.,* 139, 147-163.

Su W.-J., Woodward R.L., and Dziewonski A.M., 1994. Degree-12 model of shear velocity heterogeneity in the mantle. *J. Geophys. Res*., 99, 6945-6980.

Tan B.H., Jackson I., and Fitz Gerald J.D., 1997. Shear wave dispersion and attenuation in fine-grained synthetic olivine aggregates: preliminary results. *Geophys. Res. Lett.,* 24, 1055-1058.

Tarantola A. and Valette B., 1982. Generalized nonlinear inverse problems solved using the least squares inversion. *Rev. Geophys.,* 20, 219-232.

Trampert J. and Woodhouse J.H., 1995. Global phase velocity maps of Love and Rayleigh waves between 40 and 150 s. *Geophys. J. Int.,* 122, 675-690.

Trampert J. and Woodhouse J.H., 2000. Assessment of global phase velocity models. *Geophys. J. Int*. 142, 67-73.

Tsumura N., Matsumoto S., Horiuchi S. and Hasegawa A., 2000. Three-dimensional attenuation structure beneath the northeastern Japan arc estimated from spectra of small earthquakes. *Tectonophys.,* 319, 241-260.

Woodhouse J.H. and Wong Y.K., 1986. Amplitude, phase and path anomalies of mantle waves. *Geophys. J. R. Astron. Soc*., 87, 753-773.

Xu X., O'Reilly S.Y., Griffin W.L., and Zhou X., 2000. Genesis of young lithospheric mantle in southeastern China; an LAM-ICPMS trace element study. *J. Petrology*, 41, 111-148.